Volume 3(1),2025, Page 71-90

Geometrical Parameters Improvement of Snorkel Type Magnetic Lens Using FEMM and MELOP Programs

R.Y. J. Al-Salih1* , E. M. A. Alkattan2, , A. I. M. AlAbdullah3, Nadir F. Habubi4,5

1College of Science, Department of Physics, Tikrit University;

E-mail: r.y.jasim@tu.edu.iq

2The General Directorate for Education into Nineveh Conservative, Iraq. E-mail: ezadeenabd@yahoo.com

3College of Science, Department of Physics, Mosul University;

E-mail: abdullahidrees@uomosul.edu.iq

4Department Radiology Technologies, Al-Nukhba University College, Baghdad 10013,Iraq.

E-mail: n.fadhil@alnukhba.edu.iq

5Department of Radiology Techniques, Al-Qalam University College, Kirkuk 36001, Iraq.

ABSTRACT: A systematic study to improve optical and magnetic properties of snorkel-type magnetic lens using (FEMM) program for calculating axial magnetic field distribution using Finite Element Method (FEM) and using (MELOP) program for calculating objective focal properties of electron lenses. Two programs (FEMM & MELOP) have achieved evident success in studying, improving, and developing both magnetic and optical properties of snorkel-type magnetic electronic lenses by efficiently controlling the change of geometric parameters of these lenses.

Keywords: Snorkel magnetic lens, Lenses Geometrical parameters, Axial magnetic field distribution, Finite element method, Objective focal properties.

1. INTRODUCTION

Electron microscopy is essential for characterizing many new applications, such as Nanomaterials and other modern techniques. Their internal procedures are often highly costly and usually concealed from the user. n If researchers in fields like materials science have access to the necessary tools, this scenario can provide prompt and excellent results. The operation of inexpensive electron detectors for scanning electron microscopes (SEMs) was clarified by Vlasov et al. in 2023. They also showed that even a simple design can produce satisfactory results and offer much freedom for research and customization [1].

The SEM's required purposes, such as aperture alignment and sensor insertion/removal, are remotely retrieved through equivalent software [2]. Mahato *et al.* stated that: "Only SEM method could successfully verify all of underlying regions (Upper palisades UP, lower palisades LP, and d

mammillary region M) of the tested samples thorough imagining of these three principal regions, where they used SEM-Energy Dispersive Spectrometry system (EDS) assisting in the SEM to analyze the mineral concentration of the individual areas [3].

A high-temperature heater combined with an SEM was designed to inspect the microstructure development behavior of materials at high temperatures by Zhang *et al*.. The heat capacity of the heater was heightened by improving the structure of tungsten filament. Using a visible-light filter, a custom-built high-temperature secondary-electron detector was improved to exclude visible and infrared light. The negative influence of thermal electrons on the image quality has been resolved using a "bias-voltage controller system" [4].

In most electron beam "EB" instruments, like scanning electron microscope "SEM" instruments, a ray of EB emitted from a cathode or field emission "FE" tip is focused on a small spot area using magnetic lenses, that yields an axially field distribution. The objective lens is one at the end of the microscope's column. This lens plays a vital role in determining the final electron probe diameter. When objective lens performance is low, no accurate fine electron probe can be produced despite all efforts by components that precede the objective lens in the microscope column. Thus, designing an objective lens with best performance is vital. Three basic objective lens designs usually exist. One is called a pinhole "conical lens"; where the specimen is placed outside of lens. The second, called "immersion lens", should use a small specimens (several millimeters) inside the lens. The third is called a "snorkel lens", where its specimen should be placed outside the lens; inside its magnetic field [5]. This type of lens can works in low-voltage SEMs'. Magnetic field of snorkel lens extends outside it to reach specimen. Intensive investigations were accomplished to optimize appropriate geometrical dimensions of symmetrical dipolar (double polepiece) snorkel magnetic electron lenses by Cleaver in 1980 [6] and asymmetrical dipolar snorkel lens by Wenxiong in 1988 [7]. Optimization of polepiece shape had been studied for asymmetrical unipolar lenses by Al-Khashab and Abbas in 1991 [8]. The shape of a saturated unipolar electromagnetic lens and the effect of its size on the efficiency of unipolar electromagnetic lenses had been investigated by EL-Shahat *et al*. in 2014 [9, 10].

Al-Salih and Kalil studied the pole piece geometry influence on unipolar electromagnetic objective lens characteristics. A new design of snorkel lens with specific geometric dimensions of a square-shaped pole had been produced. Different polepiece shapes were designed, and their optical characteristics were studied. Their outcomes showed no noticeable effect of square-shaped polepieces on the properties of the objective lens [11].

In this work, a new program was written to calculate an axial magnetic field distribution (MFD) of magnetic systems using a finite element method (FEM) that can be successfully applied to electron gun designs and any new project of electron magnetic systems. The present work also aims to improve the general properties of the snorkel-type magnetic lens using "Finite Element Magnetic Method "FEMM" program [13] for calculating the axial MFD using the FEM and using "Magnetic Electron Lens Optical Properties (MELOP)" program [14] for calculating objective focal characteristics of electromagnetic lenses to make a comparison between the results of these two techniques "FEMM & MELOP" to ensure the accuracy of the performance of our new program "MELOP".

2. CALCULATIONS AND RESULTS

Computer simulators are vital in designing, optimizing, and investigating charged particle optical systems. It empowers the efficiency of such structures to be prophesied accurately before they are built. In that way, it saves time, effort, and money [15]. In addition, significant developments in computer

simulation have helped resolve a lot of complex lens designs that were difficult to implement beforehand [16].

FEM technique is usually used as a numerical technique for analyzing and drawing geometrically designed magnetic lens shapes by generating triangular finite element meshes for any suggested design to investigate their magnetic and optical properties. The most advanced technique for examining and analyzing electron lenses in analytical processes is FEM. Every mesh point is assigned a potential value, which is thought to vary linearly throughout each finite element with a triangle shape [17].

This work uses FEMM and MELOP programs to calculate axial magnetic field distribution and objective focal properties of suggested electron lenses and then compare their results. According to Munro's calculations, the software packages of booth-used programs offer design settings, field calculations, ray outlining, and valuation of needed paraxial characteristics and aberrations [18]. Munro computed booth spherical "C_s" and chromatic aberration "C_c" coefficients using Simpson's rule to evaluate the aberrations as follows [19]:

$$C_s = \frac{\zeta}{128\,.Vr}\int_{z_o}^{z_i}\left[\frac{3\zeta}{Vr}B_z^4.r_a^4(z) + 8\left(\frac{dB_z}{dz}\right)^2 r_a^4(z) \_ 8B_z^2.r_a^2(z)\left(\frac{dr_a(z)}{dz}\right)^2\right]d_z \text{ …..... (1)}$$

$$C_c = \frac{\zeta}{8\,.\,Vr}\int_{z_o}^{z_i} B_z^2.r_a^2(z)\,dz \text{ ……..……. (2)}$$

where; ζ is "charge to the electron mass ratio", V_r is "relativistic corrected accelerating voltage", B_z is "axial flux density", and $r_a(z)$ is "solution of paraxial ray equation, which is calculated using a 4th order Runge – Kutta formula [19].

2.1 DESIGNED MAGNETIC OBJECTIVE LENS AND ITS OUTCOMES

The design of magnetic lenses needs the determination of best geometrical electrode structure and their operating circumstances (operating voltage value, coil excitation value, operating method, desired focal characteristics, and any suitable shape and size of excited coil built-in) [20].

Figure (1) below shows a simple diagram of upper half of the suggested Snorkel lens in the present work with its geometrical dimensions and other parameters. It appears that the model is rotationally symmetrical. It has an axial length of (70 mm), radial width of (180 mm), a sectional area of coil (1000 mm^2), air gap of (s = 15 mm), polepiece snot face of (10 mm), diameter of axial bore (D_p = 6 mm), cylindrical gap of (40 mm) diameter, and (50 mm) length.

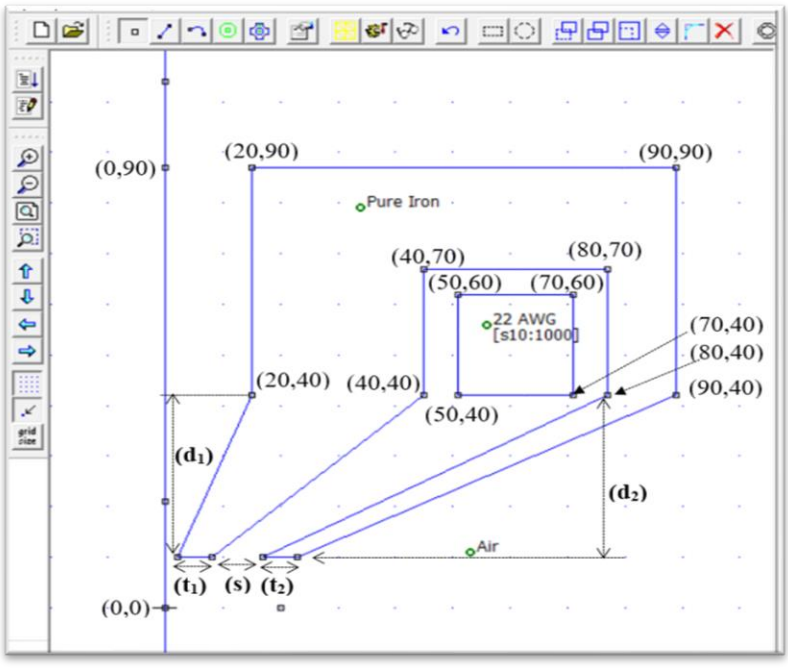

2.2 EFFECT OF AIR GAP BETWEEN THE FACES OF POLES AND THE IRON SHROUD (s)

To determine the efficiency of the proposed objective magnetic lenses illustrated in Figure (1); FEMM program has computed the designed lens's axial magnetic flux density distribution. Figure (2) illustrates The axial magnetic field distribution of the lens at altered values of (s) that were calculated at fixed excitation value (NI =10 kA.t) for designed lens as a function of axial distance. The last Figure (Fig. 2) shows that the magnetic flux peak and distribution shape depend on geometrical design of lens. It is found that the distribution of magnetic flux density of suggested lens is regular with a bell-shaped form, so it has a maximum value at the center of air gap; where the sample is placed outside of magnetic field; where the aberration coefficients magnitudes will ordinary predictable to be of high values [21]. Ali *et al.* studied the effect of crucial geometric factors. They found that its importance comes from its ability to determine the appropriate geometry of magnetic lenses, thus assisting their effectual request. They stated that the air gap plays a vital role in attaining the optimal design of a magnetic lens, and objective focal characteristics showed extensive development with the reduction in air gap. So, the levitation air gap of such lens marks in a broadening of half-width of axial magnetic field concurrently causes a decrease in maximum magnetic field magnitude [22].

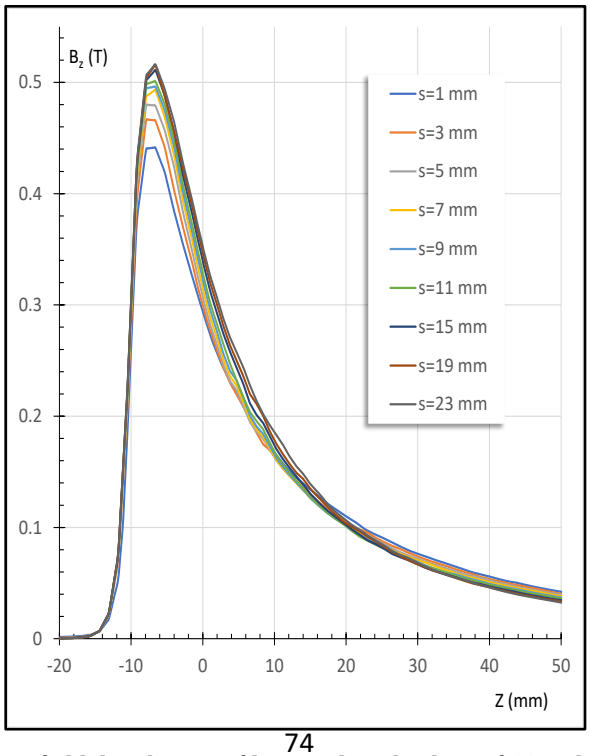

Figure 2: Axial magnetic field distribution of lens at altered values of (s); calculated at fixed excitation value of (NI = 10 kA.t) using FEMM program.

Figure (3) illustrates magnetic flux density plots of lens at altered values of (s); calculated at fixed excitation value of (NI = 10 kA.t) using FEMM program.

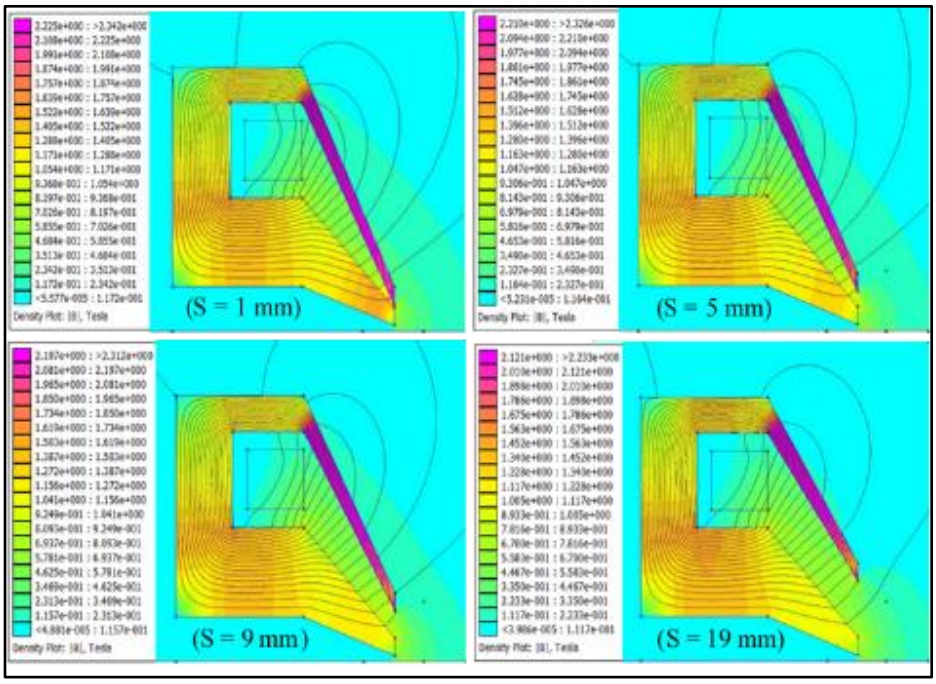

Figure 3: Magnetic flux density plots of lens at altered values of (s); calculated at fixed excitation value of (NI=10 kA.t) using FEMM program**.**

It is clear from the last Figure (3) that the air gap (s) dramatically affects the distribution of the magnetic flux density. Ali *et al*. studied the usefulness of magnetic lenses by employing Electron Optical Design. Their investigation focused on the effect of essential geometric dimensions, precisely "air gap (s)" on objective and projector characteristics. They ensured that it is necessary to choose a suitable geometry for magnetic lenses, especially the air gap factor, thereby facilitating their efficient application [22].

Figure (4) below shows the variation of objective focal properties (C_s, C_c, f_o) with accelerating voltage of lens at changed values of (s); computed at fixed excitation value of (NI =10 kA.t) using MELOP program.

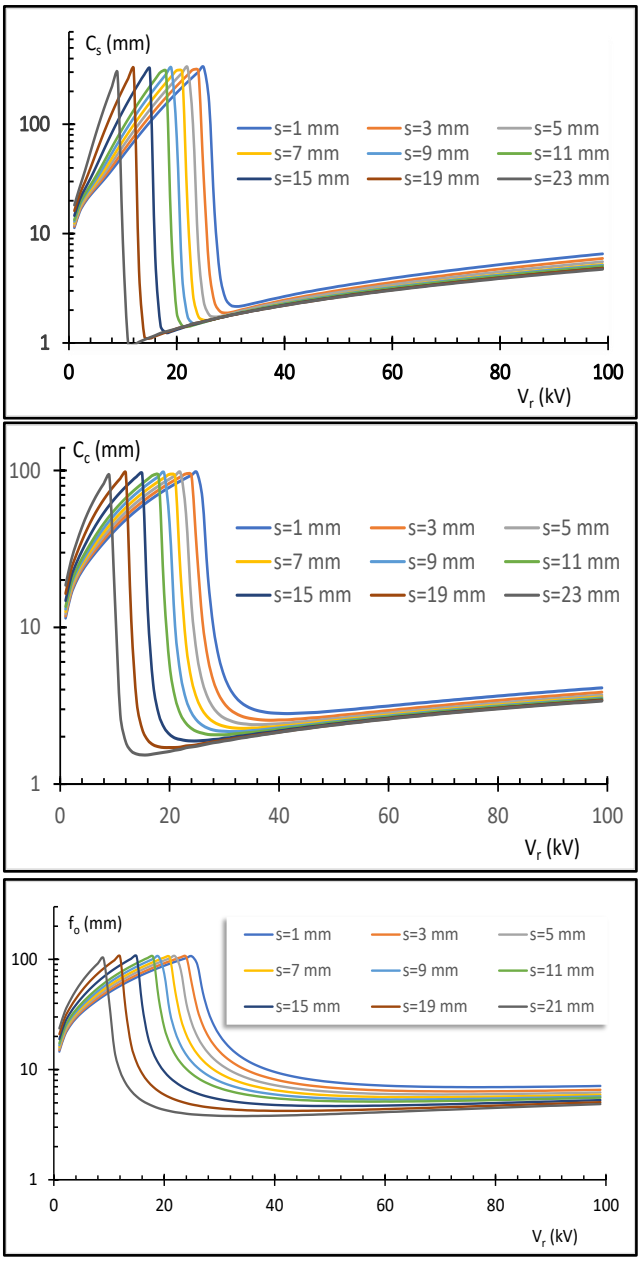

Figure 4: Variation of objective focal properties (C_s , C_c , f_o) with accelerating voltage of lens at altered values of (s); calculated at fixed excitation value of (NI=10 kA.t) using MELOP program**.**

2.3 DETERMINATION OF THE OPTIMUM FACE THICKNESS OF POLRPIECE AND IRON SHROUD IN DESIGNED LENSES

For constant ratio: (r =1) when ($t_1 = t_2 = t$), the axial MFD of lens at altered values of (t); calculated at fixed excitation value of (NI =10 kA.t) using FEMM program will appear the characteristics shown in Figure (5) below.

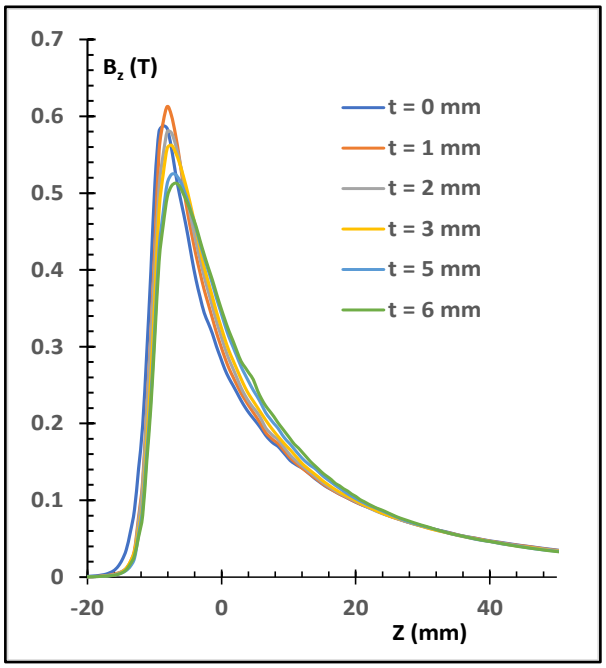

Figure 5: Axial MFD of lens at altered values of (t); calculated at fixed excitation value of (NI = 10 kA.t)

A comparison between values of B_{max} and HW of lens at altered values of (t) calculated at a fixed excitation value of (NI = 10 kA.t) has been shown in Figure (6).

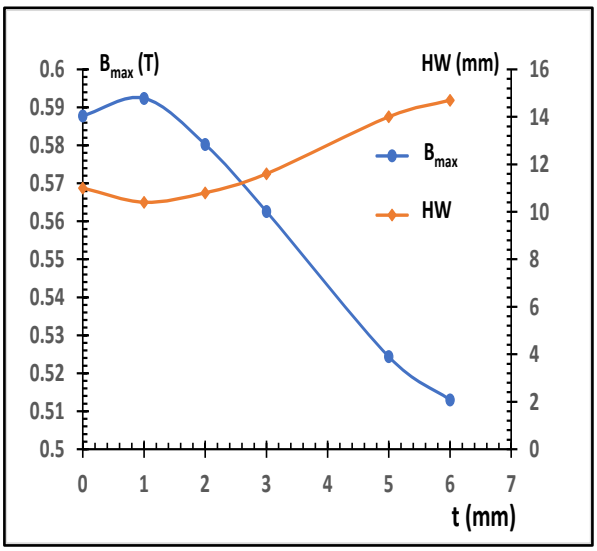

Figure 6: Comparison between values of Bmax, and HW of lens at altered values of (t); calculated at fixed excitation values of (NI =10 kA.t)

Variation of objective focal characteristics (C_s, C_c, f_o) with relatively accelerating corrected voltage of lens at altered values of (t), calculated at fixed excitation value (NI =10 kA.t) using MELOP program has been played as demonstrated in Figure (7).

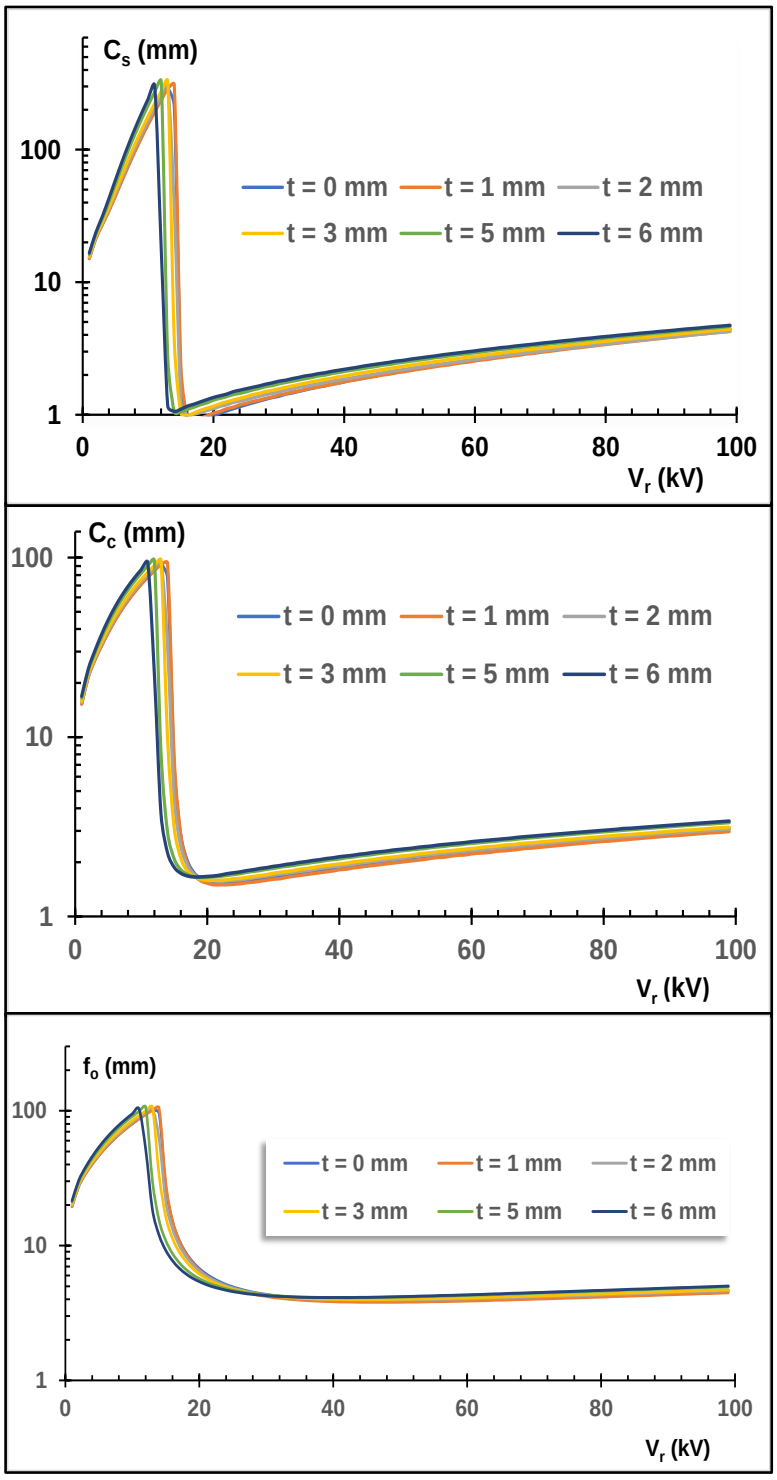

Figure 7: Variation of objective focal properties (C_s, C_c, f_o) with accelerating voltage of lens at altered values of (t) calculated at fixed excitation value of (NI =10 kA.t) using MELOP program.

Figure (8) below clears the magnetic flux density plots of the lens at altered values of (s); calculated at a fixed excitation value of (NI =10 kA.t) using FEMM program.

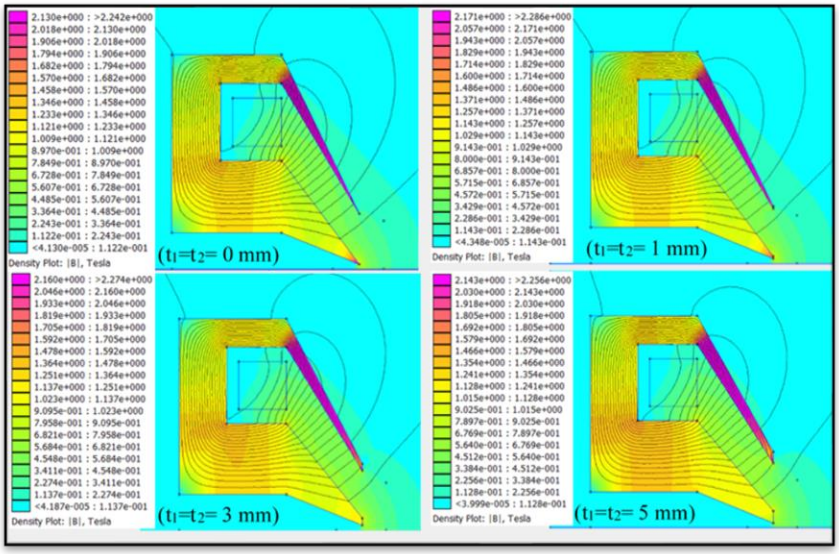

Figure 8: Magnetic flux density plots of lens at altered values of (s); calculated at fixed excitation value of (NI =10 kA.t) using FEMM program.

In the case of (t_1 = t_2 = t), Figures (7,8) show that the best ratio for the face thickness of the polepiece and the iron shroud in the lens attended at the values (t = 1, r =1) where the lens acquired highest value of B_{max} and lowest value of half-width.

Another investigation for variable ratios (r =0.5 – 50) had been done, and the resultant of these values are illustrated in Figure (9), where axial magnetic field distribution of lens has been studied at altered values of (r) calculated at fixed excitation (NI=10 kA.t) using FEMM program.

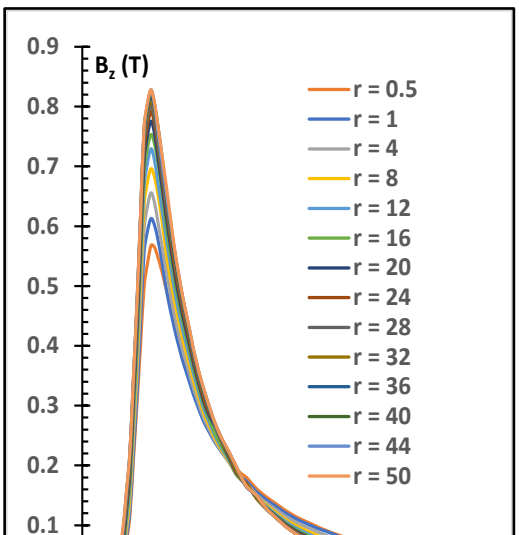

Figure (10) illustrates a comparison between values of B_{max}, and HW of lens at altered values of (t); calculated at a fixed excitation value of (NI =10 kA.t). In contrast, Figure (11) represents the variation of objective focal properties (C_s , C_c , f_o) with accelerating voltage of lens at different values of (r); calculated at fixed excitation value of (NI =10 kA.t) using MELOP program.

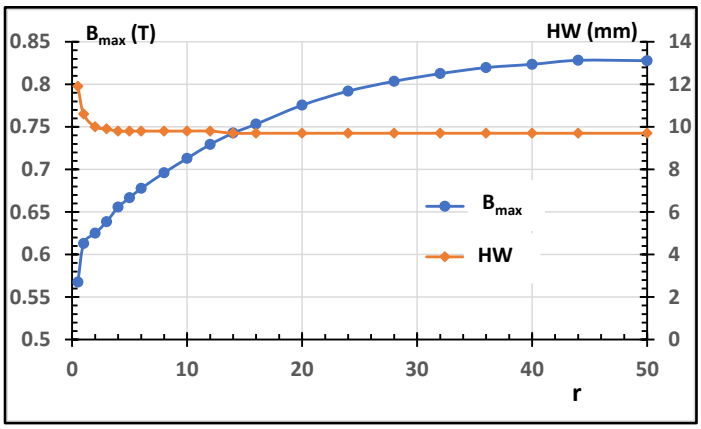

Figure 10: Comparison between values of B_{max}, and HW of lens at altered values of (t); calculated at fixed excitation value of (NI =10 kA.t).

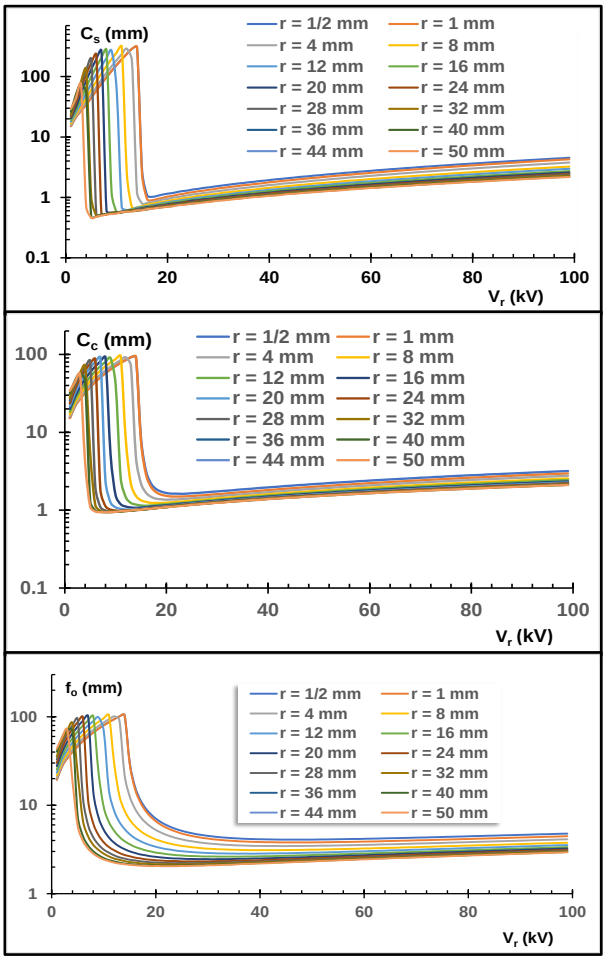

Figure (12) demonstrates the magnetic flux density plots of lens at altered values of (r); calculated at a fixed excitation value of (NI = 10 kA.t) using FEMM program.

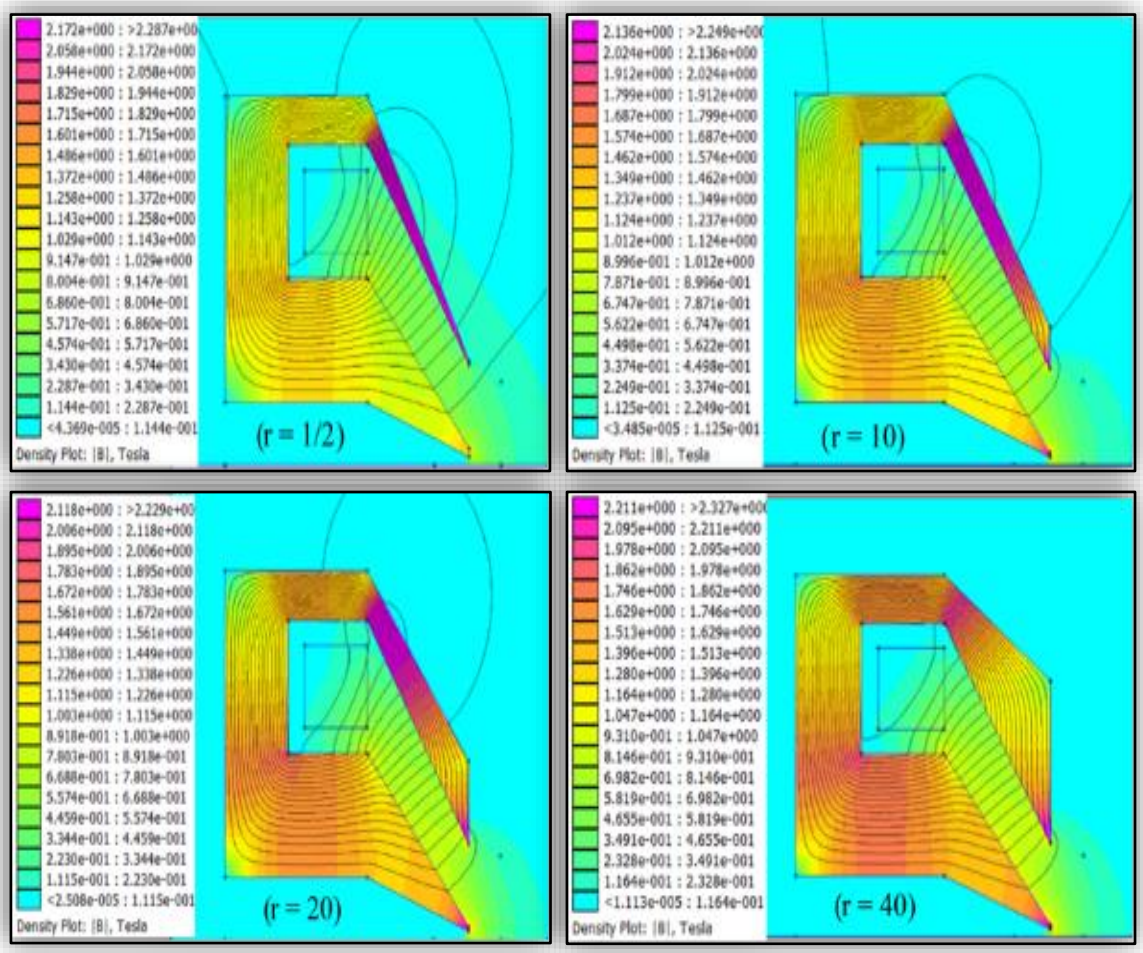

Figure 12: Magnetic flux density plots of lens at altered values of (r); calculated at fixed excitation value of (NI = 10 kA.t) using FEMM program.

It is found that from Figures (11,12) (in case of $r = t_2/t_1$), the best ratio for the face thickness of the polepieces in lens attended at values of ($r > 40$) where lens acquired highest value of B_{max} and lowest value of half-width.

2.4 DETERMINATION OF THE BEST POSITION OF POLEPIECE AND IRON SHROUD

Another study is in the case of (d1 = d2 = d); where d1 & d2 are the lengths of polepiece and iron shroud, respectively. Figure (13) illustrates axial MFD of the lens for the last case at altered values of (d); calculated at fixed excitation value of (NI = 10 kA.t) using FEMM program.

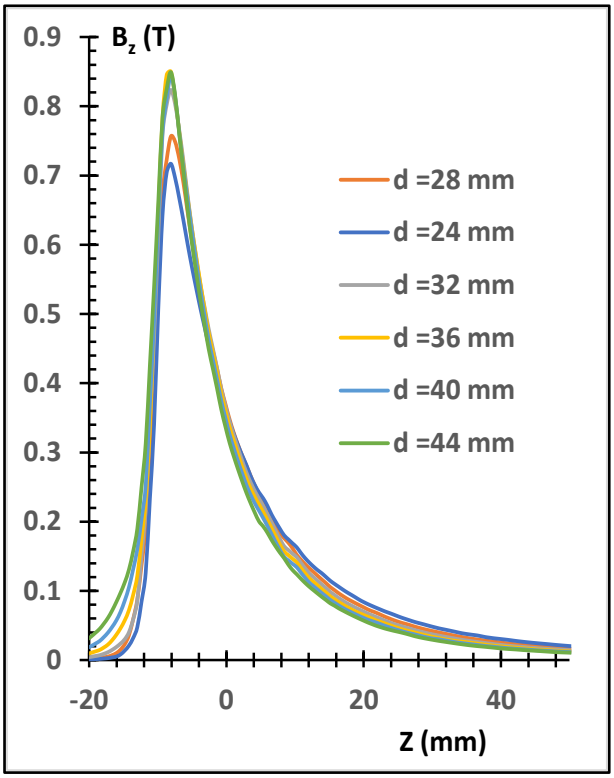

Figure 13: Axial magnetic field distribution of lens at altered values of (d); calculated at fixed excitation value of (NI = 10 kA.t) using FEMM program.

Figure (14) shows a comparison between values of B_{max}, and HW of lens at altered values of (d); calculated at a fixed excitation value of (NI = 10 kA.t). The best resultant seems to have been achieved at (d= 36 mm).

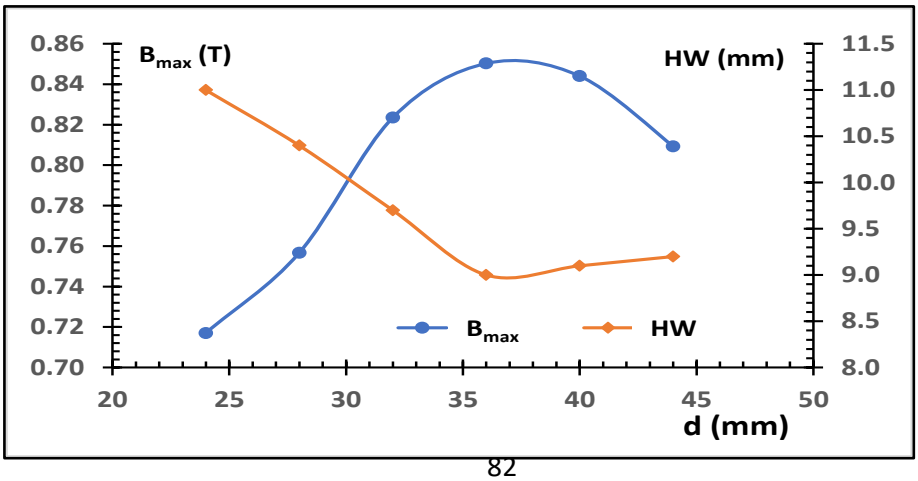

Figure 14: Comparison between values of B_{max}, and HW of lens at altered values of (d); calculated at fixed excitation value of (NI = 10 kA.t)

Variation of objective focal parameters (C_s, C_c, f_o) with accelerating voltage of lens at altered values of (d); calculated at fixed excitation value of (NI = 10 kA.t), has also been investigated using MELOP program. as shown in Figure (15). It is found that the best properties were achieved at a value of (d= 36 mm.(

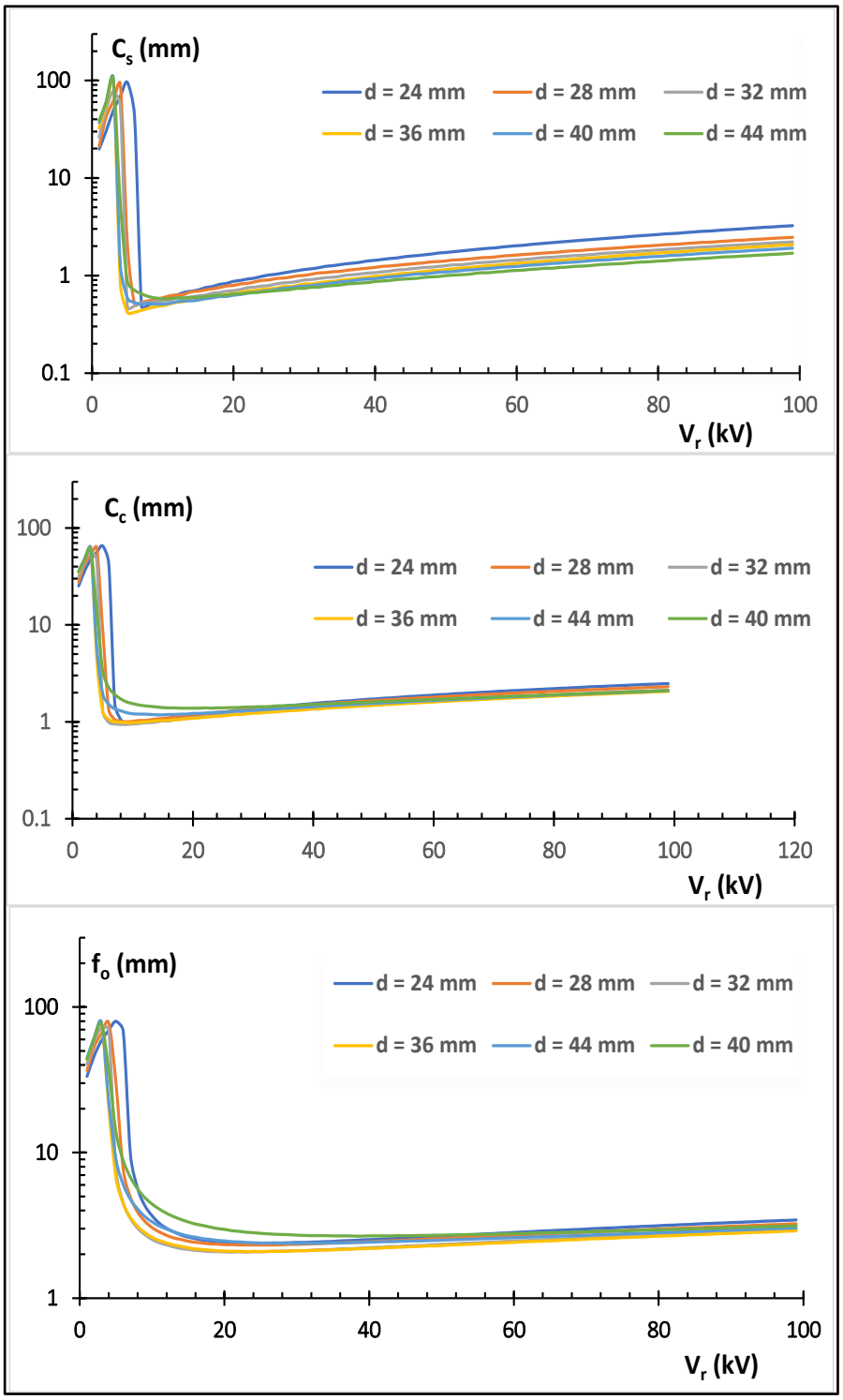

Figure 15: Variation of objective focal parameters (C_s, C_c, f_o) with accelerating voltage of lens at altered values of (d); calculated at fixed excitation value of (NI = 10 kA.t) using MELOP program.

Another study has been done in case of (D= d2/d1). The result of this study is shown in following figures at altered values of (D = 0.66, D = 0.77, D = 0.88, D = 1.00, D = 1.11, D = 1.22, and D = 1.33). Figure (16) shows axial magnetic field distribution of lens at altered magnitudes of (D); calculated at a fixed excitation value of (NI = 10 kA.t) using FEMM program. Polepiece geometry has a vital influence on the performance of magnetic objective lens. AL-Bayati and Al-Salih designed and investigated a newly invented immersion magnetic lens. They found that lens with a thickness of (D = 10 mm) of iron back plate achieved finest results among suggested designs, because it had lowest values of focal length due to highest values of magnetic field, so spherical and chromatic aberration coefficients also had been decreased [23]. A different design of snorkel lens with alternate geometric parameters of square polepiece shape was produced and studied by Al-Salih and Kalil in 2024. They confirmed that the shape of polepiece geometry significantly affects the performance of electromagnetic objective lens [11].

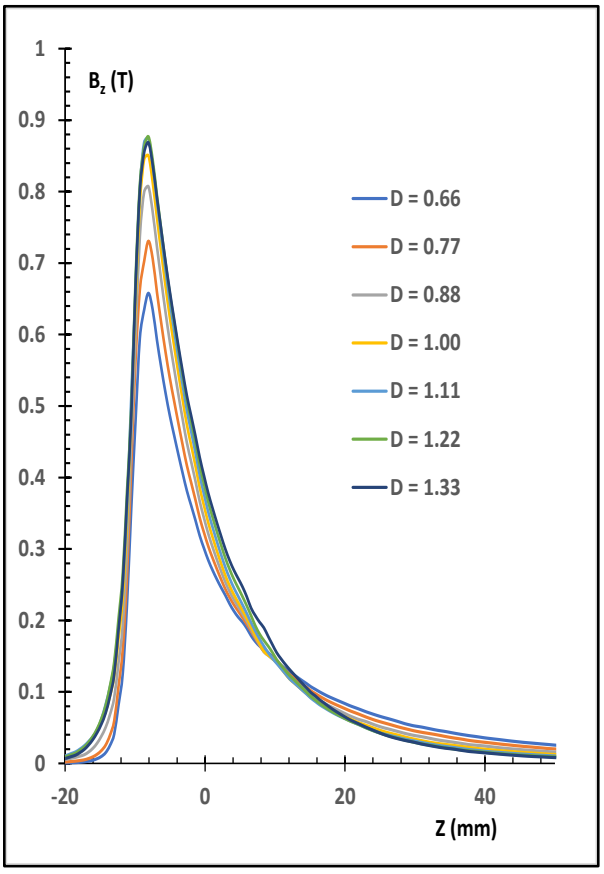

Figure 16: Axial magnetic field distribution of lens at altered values of (D); calculated at fixed excitation **value**

Figure (17) illustrates a comparison between the values of B_{max}, and HW of lens at altered values of (D); calculated at a fixed excitation value of (NI = 10 kA.t).

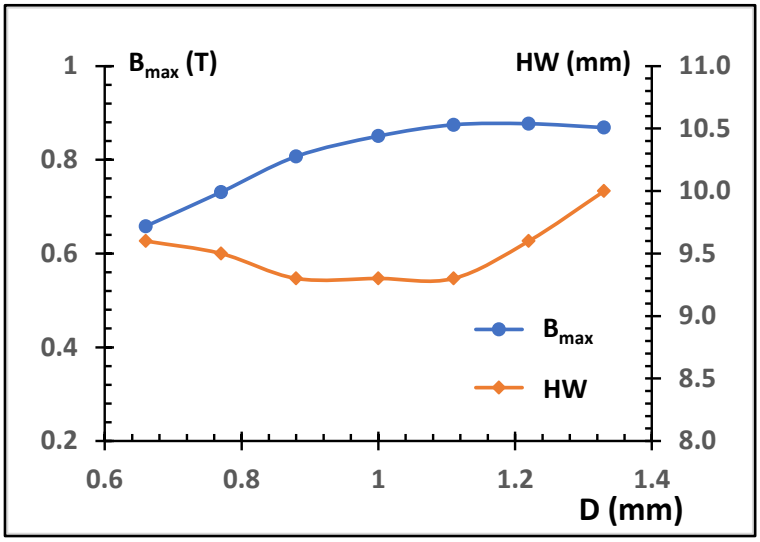

Figure 17: Comparison between values of B_{max}, and HW of lens at altered values of (D); calculated at fixed excitation value of (NI = 10 kA.t).

Changing of objective focal parameters (C_s, C_c, f_o) with accelerating voltage of the lens at altered values of (D); calculated at fixed excitation value of (NI = 10 kA.t) using MELOP program. The consequences are illustrated in Figure (18). It is found that the best value has been obtained at D = 1.22 mm.

The outcome results in the present work are compatible with Al-Salih and Janan, who found that magnetic flux density increases when the inner bore diameter. In addition, results showed that spherical chromatic and aberration factors (C_s, C_c) decrease with decreasing inner bore diameter to obtain better optical characteristics [24].

The current study's findings align with those of Musa and Abbas, who discovered that the imaging field is more significantly affected by changes in the axial bore diameter (D), particularly at the extremities of the optical axis. Therefore, increasing the axial bore diameter (D) of a single-pole piece magnetic lens causes the axial magnetic field's half-width to increase, accompanied by a drop in the magnetic field's maximum value. Additionally, the slope of the electron beam trajectory as it enters the lens decreases as the axial bore diameter (D) of the single-pole piece magnetic lens increases. Lastly, to achieve appropriate objective optical qualities, a small number of axial bore diameter (D) values should be selected [17].

Janan and Al-Salih also discovered that MFD rises when inner bore diameter falls. Therefore, as the inner bore diameter decreases, the chromatic and spherical aberration factors also decrease, improving the optical properties. The maximum flux density increases as current density rises while resolving power (δ) improves and aberration factors fall. Additionally, it has been discovered that a

magnetic field will grow (Bz = 0.18 Tesla) when the current density is increased by two values (2 A/mm^2) [25].

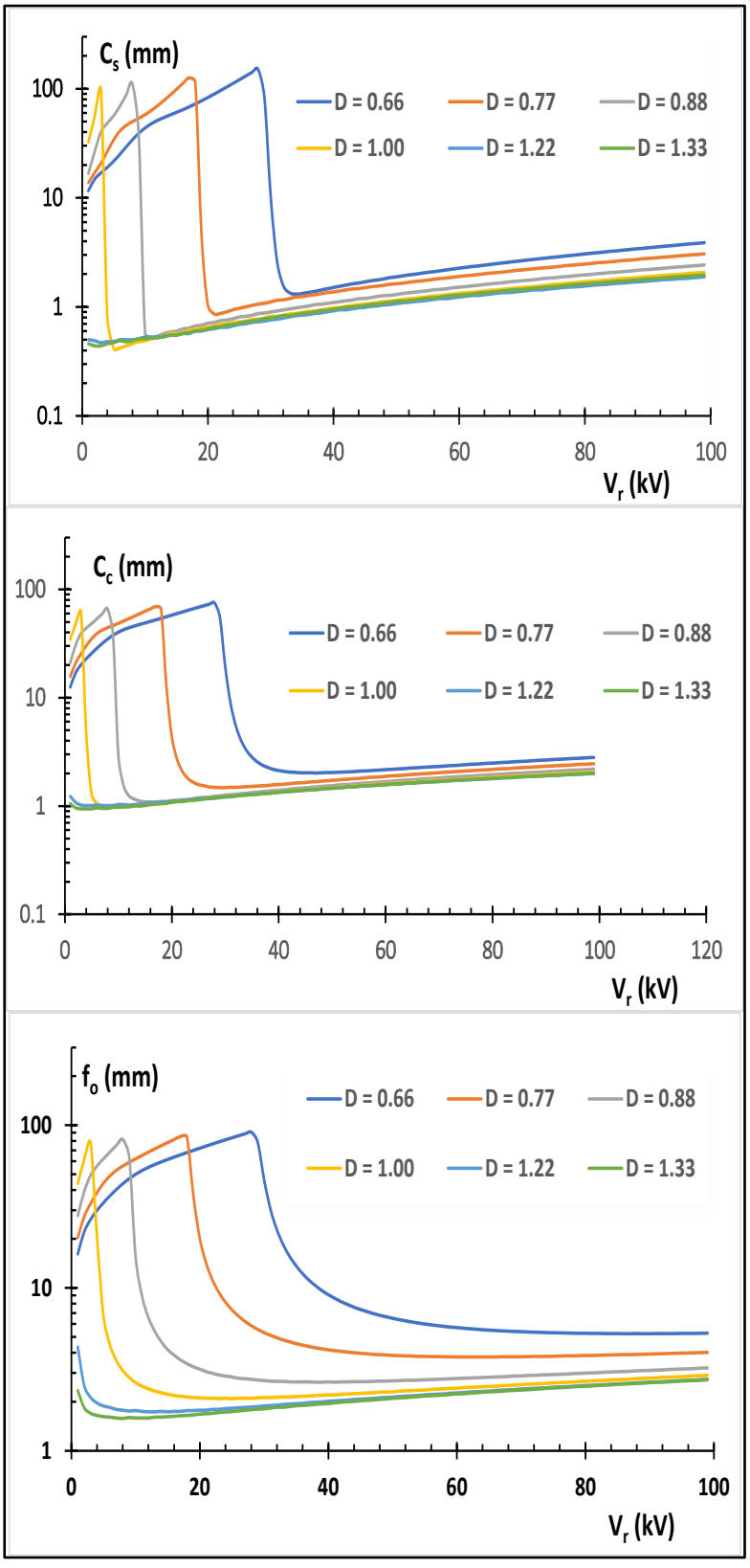

Figure 18: Variation of objective focal properties (C_s, C_c, f_o) with accelerating voltage of lens at altered values of (D); calculated at fixed excitation value of (NI = 10 kA.t) using MELOP program.

2.5 USING ROUNDED EDGES INSTEAD OF ANGLES

FIMM program allows the use of arc segments in the design of magnetic circuits. Investigations are carried out to demonstrate the effect of adopting rounded edges for magnetic circuits instead of conventional angled shapes. Comparison between lens magnetic flux density plots in the case of rounded edges and traditional design, calculated at a fixed excitation value of (NI = 10 kA.t) using FEMM program, is demonstrated in Figure (19).

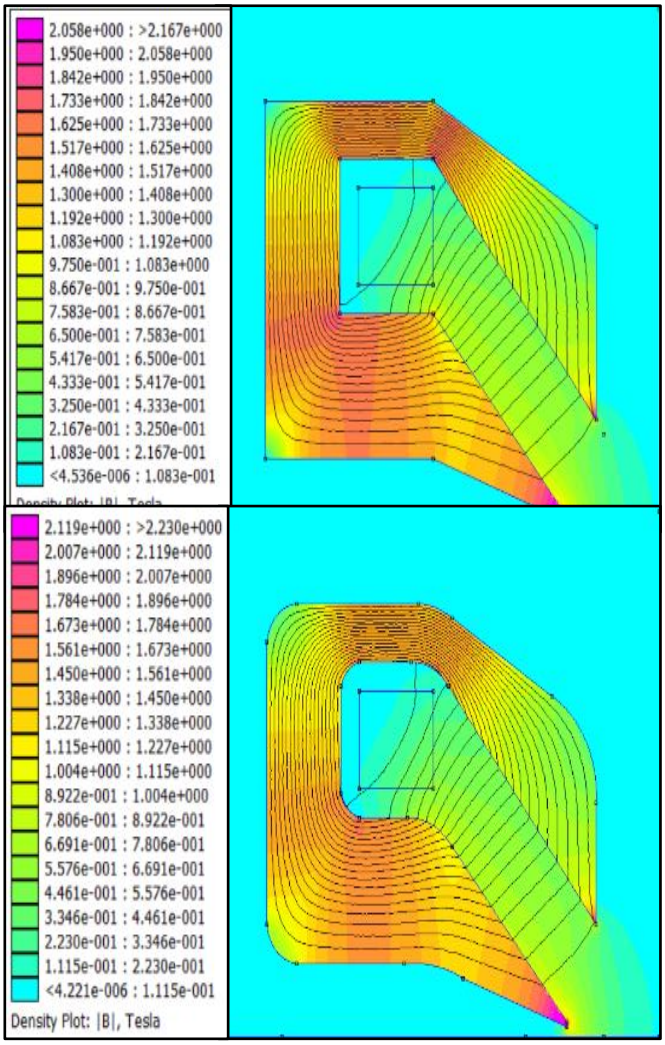

Figure 19: Comparison between magnetic flux density plots of lens in case of rounded edges and the conventional design; calculated at fixed excitation value of (NI = 10 kA.t) using FEMM program.

Axial magnetic field distribution of lens shapes with rounded and conventional angled edges calculated at a fixed excitation value of (NI = 10 kA.t) using FEMM program is shown in Figure (20). It also seems that axial magnetic field distributions of two lenses match entirely, i.e.: iron circuit

has a limited effect on lens properties, and its performance depends mainly on the critical polepiece region.

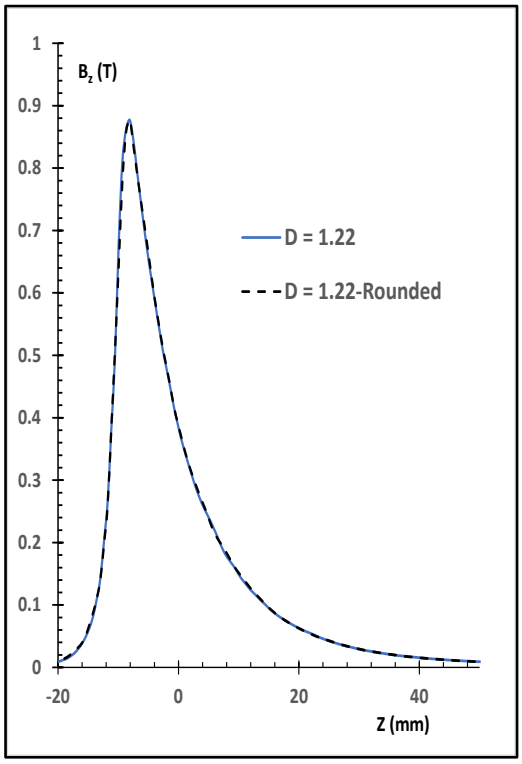

Figure 20: Axial magnetic field distribution of lens shapes with rounded and conventional angled edges, calculated at fixed excitation value of (NI = 10 kA.t) using FEMM program.

3. CONCLUSIONS

A systematic study to improve the optical and magnetic properties of the snorkel-type magnetic lens using (FEMM) program for calculating the axial magnetic field distribution using Finite Element Method and the "MELOP" program to calculate the objective focal properties of electromagnetic lenses. It was found that the two programs (FEMM & MELOP) have achieved evident success in studying, improving, and developing both magnetic and optical properties of snorkel-type magnetic electronic lenses by efficiently controlling the change of geometric parameters of these lenses.

REFERENCES

1. Vlasov, E., Denisov,N., Verbeeck, J., "Low-cost electron detector for scanning electron microscope", HardwareX 14 (2023) e00413.
2. Lang, E.J., Heckman N.M., Clark, T. , Derby, B., Barrios, A. , Monterrosa, A., Barr a , D.L. Buller, C.M., Stauffer, D.D., Li N., Boyce, B.L., Briggs, S.A., Hattar, K., "Development of an in situ ion

irradiation scanning electron microscope", Nuclear Inst. and Methods in Physics Research, B 537 (2023) 29–37.

3. Mahato, P.L. , Weatherby, T., Ewell, K., Jha, R. , Mishra, B., "Scanning electron microscope-based evaluation of eggshell quality", Poultry Science, (2024). 103:103428.
4. Zhang, Y., Tang L. , Wang Y. , Wang, J., Zhou, J., Lu,J., Zhang, Y., Zhang, Z., "Development and application of a high-temperature imaging system for in-situ scanning electron microscope", Materials Today Communications 38 (2024) 107782.
5. Goldstein, J; Newbury, D. E.; Joy, D. C.; Lyman, C. E.; Echlin, P.; Lifshin, E.; Sawyer, L. C.; Michael, J. R., "Scanning electron Microscopy and X-Ray Microanalysis", 3rd Edition, Kluwer Academic / Plenum Publishers. New York, (2003).
6. Cleaver, J. R. A., "The choice of polepiece shape and lens operating mode for magnetic objective lenses with saturation polepiece", *Optik*, **57**, 9-34, (1980).
7. Hamad, A. A., Khalil, M. M., Al-Obeidi, A. S., Al-Azzawi, S. F., & Thivagar, L. (2024). Complex networks applied to the analysis of the dynamics of social systems. International Journal of Grid and Utility Computing, 15(1), 97-103.
8. Al-Khashab, M.A. ; Abbas, I.K., "Optimized polepiece shape for asymmetrical single polepiece magnetic electron lenses", *Modeling, Simulation and Control*, A. AMSE Press, **35**(3), 1-9, (1991).
9. EL-Shahat, S. S.; Al Amir, A. S. A.; Hassan, G. S., "Studies on the effect of pole piece shape for saturated single pole magnetic lens", *Proceedings of the 1st International Conference on New Horizons in Basic and Applied Science, Hurghada* – Egypt, **1**(1), 290-298, (2014 a).
10. EL-Shahat, S. S.; Hassan, G. S.; Al Amir, A. S. A., "The effect of lens size on performance Single Pole Magnetic Lens", *Journal of Scientific Research in Physical & Mathematical Science*, **1**(5), 2349-7149, (2014 b).
11. Al-Salih, R. Y. J., & Kalil, N. K. "Effect of polepiece geometry on objective snorkel lens properties". *Fifth International Conference on Applied Sciences*, *AIP Conference Proceedings*, *3097*(1), (2024).
12. Alabdullah, A. I. M., Alkattan, E. M. A., Al-Salih, R.Y. J., "Program for Calculating the Axial Magnetic Field Distribution of Magnetic Lenses Using Finite Element Method", *Jordan Journal of Physics* **16**(5), 551-561, (2023).
13. Meeker, D. C., Finite Element Method Magnetics., "User's Manual", October 25, (2015).
14. Al-Salih, R.Y.J., Al-Abdulla, A. I.M., Alkattan, E.M.A., "Simple program for computing objective optical properties of magnetic lenses",*Int. J. Computer Applications in Technology*, **66** (3/4), 254- 259, (2021).
15. Munro, E., "Munro's electron beam software MEBS", Report, MEBS Ltd., London SW74AN, England, (2011).
16. Abbass, T.M. ; Nasser, B.A., "Study of the objective focal properties for asymmetrical double polepiece magnetic lens", *British Journal of Science*, **6**(2), 43-50, (2012).
17. Musa, S. J., Abbas, T. M., "Design and investigate the optical characteristics of single polepiece magnetics lenses", Materials Today: Proceedings 80 (2023) 2307–2314.
18. Munro, E., "A Set of Computer Programs for Calculating the Properties of Electron Lenses", Cambridge University, Eng. Dept., Report CUED/ ELECT/TR 45, (1975).
19. Nakagawa, S.; Miyokaum, T.; Noguchi, Y., "Axial magnetic corrected field lens (C-F lens)-principle and characteristics, minimizing Cs and Cc", *Electron Microscopy*, **1**(3). 901-909, (1980).
20. Al-Khashab, M.A ; Al-Hialey, R. W., "The effect of geometrical shape and

position of the coil on optical performance for asymmetrical magnetic lens", *Rafidain journal of science*, **24**(2), 91-100, (2013).

21. Mulvey, T., "Unconventional lens design in Magnetic Electron Lenses", Ch.5, Ed. Hawkes, P.W., Springer-Verlag, Berlin, 359-420, (1982).
22. Ali, R. SH., Hussein, M. A., and Al-Salih, R.Y.J., "Optimizing the Effectiveness of Magnetic Lenses by utilizing the Electron Optical Design (EOD) Software" Engineering, Technology & Applied Science Research, **13**(6), 11980-11984, (2023).
23. AL-Bayati, O. M. A., and Al-Salih, R. Y. J., "Effect Thickness Back Plate on the properties Immersion Magnetic Lens", A Journal for New Zealand Herpetology, **12**(2),487- 495, (2023).
24. AL-Salih, R. Y. J., and AL- Janan, M. K. A., "Design and Studying the Effect of Inner Bore Diameter of Unipolar Lens", Al-Mustansiriyah Journal of Science, **33** (3), 82-86, (2022).
25. Janan, M. K. A., and Al-Salih, R. Y. J., "Design and study the effect of inner bore diameter on the magnetic and optical properties of the unipolar lens", Baghdad Science Journal, 20(3): 805-814, (2023).